Phase Identification in a Series of Liquid Crystalline TPP Polyethers and Copolyethers Having Highly Ordered Mesophase Structure. 5. Solid State ^{13}C NMR Characterization of Motion and Conformations of Methylene and Mesogen Groups in Different Mesophases of TPP(n = 12 and 15)

Jinlong Cheng*

Raychem Corporation, 300 Constitution Drive, Menlo Park, California 94025-1164

Yeocheol Yoon, Rong-Ming Ho, Mark Leland, Mingming Guo, and Stephen Z. D. Cheng*

Maurice Morton Institute of Polymer Science and Department of Polymer Science, The University of Akron, Akron, Ohio 44325-3909

Peihwei Chu and Virgil Percec

Department of Macromolecular Science, Case Western Reserve University, Cleveland, Ohio 44106-2699

Received February 7, 1997; Revised Manuscript Received May 27, 1997[⊗]

ABSTRACT: Two liquid crystalline polyethers based on 1-(4-hydroxy-4′-biphenylyl)-2-(4-hydroxyphenyl)-propane and 1,12-dibromododecane and 1,15-dibromopentadecane [TPP(n = 12 and 15)] have been characterized to examine the molecular motion and conformations of the methylene units and mesogenic groups using solid state ^{13}C NMR. The methylene conformations were studied as a function of temperature by the γ-gauche effect in the ^{13}C NMR chemical shift, which depends largely on the C−C conformation under the condition of magic angle spinning. The variable-temperature NMR results on the conformational order of the methylene units may be correlated with the entropy changes in the methylene units that are associated with phase transitions measured by differential scanning calorimetry experiments. Both the entropy change of the methylene units and ^{13}C NMR chemical shift show that in the highly ordered liquid crystalline phases of this series of polyethers, the methylene units play an important role in maintaining the order of these phases.

Introduction

The liquid crystalline phase behavior of a series of polyethers synthesized from 1-(4-hydroxy-4′-biphenylyl)-2-(4-hydroxyphenyl)propane and α,ω-dibromoalkanes (TPP-n) has been identified through structural analysis, thermodynamic properties, and liquid crystalline morphology. The wide angle X-ray powder and fiber diffraction (WAXD), electron diffraction (ED), polarized light and transmission electron microscopy (PLM and TEM), and differential scanning calorimetry (DSC) experiments show that these polymers form highly ordered smectic F (S_F) and smectic crystal G and H (SC_G and SC_H) phases. All of the transitions are enantiotropic and cooling rate independent.[1−5]

Review of the enthalpy and entropy changes for the phase transitions reveals an important fact.[2,3] For TPP(n = odd)s the contribution of the mesogenic group to the enthalpy and entropy changes at the transitions of $S_F \leftrightarrow SC_G$ and $SC_G \leftrightarrow SC_H$ are practically zero. A similar observation can also be found for TPP(n = even)s at the transitions of $SC_G \leftrightarrow SC_H$. On the other hand, the contribution of the methylene units in the spacer to the enthalpy and entropy changes at these transitions appears to predominate. These observations suggest that a better understanding of the mesophase transition behavior may be critically associated with an investigation of the motion and conformational changes of the methylene units and mesogenic groups.

Solid state ^{13}C NMR spectra measured under the condition of magic angle spinning (MAS) and dipolar proton decoupling show sufficiently high resolution and permit distinction of carbon atoms by assuming different conformations along the spacer. The chemical shift of the ^{13}C nucleus using the γ-gauche effect can be utilized to determine the conformation.[6−8] In previous work, solid state ^{13}C NMR has been applied to study a series of main chain liquid crystalline polymers containing methylene units such as polyethers synthesized from 1-(4-hydroxyphenyl)-2-(2-methyl-4-hydroxyphenyl)ethane and α,ω-dibromoalkanes (MBPEs)[9] and polyesters synthesized from bis(4-hydroxyphenoxy)-p-xylene and 1,11-dibromoundecane (HPX-C11).[10] The methylene units in these polymers have been identified to possess conformational disorder in the liquid crystalline state. However, the motion and conformations of these methylene units are far from isotropic or liquid-like. The chemical shift in high-resolution MAS NMR spectra for particular carbon atoms in the methylene sequence show interesting upfield changes as a function of temperature, while the chemical shift of the remaining methylene carbon atoms in this sequence remains constant.

In this work, we attempt to study the temperature dependence of the ^{13}C chemical shift of the methylene atoms in TPP(n = 12 and 15). A semiquantitative analysis for determining the conformational order of the methylene units in each phase will be employed. This analysis is based on precise measurements of the chemical shifts and spin populations (signal intensities) of distinguishable resonances that are attributed to

* To whom correspondence should be addressed.
⊗ Abstract published in *Advance ACS Abstracts,* August 1, 1997.

S0024-9297(97)00177-0 CCC: $14.00

different conformations. The results will then be correlated with the entropy changes at various phase transitions.

Experimental Section

Materials. TPPs were synthesized from 1-(4-hydroxy-4′-biphenyl)-2-(4-hydroxyphenyl)propane and α,ω-dibromoalkanes. The detailed synthetic procedure has been reported in an earlier publication.[11] The chemical structures of these two polyethers are

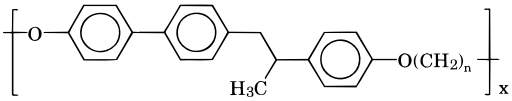

where $n = 12$ or 15. The number average molecular weights were 25 000 and 28 000, and the polydispersities were 2.6 and 2.7, respectively, as determined by gel permeation chromatography (GPC) in chloroform based on polystyrene standards.

Equipment and Experiments. The solid-state ^{13}C NMR experiments were carried out on a Chemagnetics CMX200 spectrometer, operating at 50 MHz for ^{13}C, with a 7.5 mm coaxial variable-temperature MAS probe. The variable contact time (VCT) experiments, in which a number of contact times were used for cross-polarization, were performed at temperatures between 23 and 190 °C. The contact times for each VCT experiment range from 0.01 to 20 ms. The 90° pulse width for ^{1}H in the VCT experiment was 3.5 μs, and the spin-lock field was about 42 kHz. The sample spinning speed was regulated at 4005 ± 5 Hz for all measurements. About 600 acquisitions were averaged for each spectrum. The spectra of the isotropic melts were obtained with magic angle spinning, single pulse excitation, and dipolar proton decoupling.

Differential scanning calorimetry (DSC) experiments were carried out in a Perkin-Elmer DSC-7. The temperature and heat flow scales at different cooling and heating rates (2.5−40 °C/min) were carefully calibrated using standard materials. Typically, the DSC sample size was 2−3 mg. When fast cooling and heating rates were applied the sample weight was reduced to less than 0.5 mg to avoid the formation of a thermal gradient within the samples. When the DSC cooling curves were used to analyze the transition behavior, the onset temperature of the transition on the high-temperature side was determined. The analysis also required recognition of the peak temperatures. When the peaks were overlapped, they were resolved using PeakFit published by Jandel Scientific. An asymmetric double sigmoidal function was used for the peak resolution. The equilibrium thermodynamic properties for each transition were obtained by extrapolating the experimental transition temperatures and enthalpy changes to an infinitely slow cooling rate (0 °C/min cooling rate). The entropy changes were calculated from the ratios of the enthalpy changes to transition temperatures.

Results and Discussion

Thermodynamic Properties of the Phase Transitions. The structure identification of the transitions in these two TPP polyethers has been reported in our previous publications.[2,3] The thermodynamic properties corresponding to each transition are based on the observations from DSC experiments. The transition sequences of both TPP polyethers are listed as follows:

$$\mathrm{I} \xleftarrow[18.14\ \mathrm{kJ/mol}]{150\ ^\circ\mathrm{C}} \mathrm{S_F} \xleftarrow[6.21\ \mathrm{kJ/mol}]{130\ ^\circ\mathrm{C}} \mathrm{SC_G} \xleftarrow[13.69\ \mathrm{kJ/mol}]{118\ ^\circ\mathrm{C}} \mathrm{SC_H} \xleftrightarrow{23\ ^\circ\mathrm{C}} T_g$$

for TPP($n = 15$), and

$$\mathrm{I} \xleftarrow[18.84\ \mathrm{kJ/mol}]{184\ ^\circ\mathrm{C}} \mathrm{S_F} \xleftarrow[6.45\ \mathrm{kJ/mol}]{165\ ^\circ\mathrm{C}} \mathrm{SC_G} \xleftarrow[11.20\ \mathrm{kJ/mol}]{148\ ^\circ\mathrm{C}} \mathrm{SC_H} \xleftarrow[2.96\ \mathrm{kJ/mol}]{128\ ^\circ\mathrm{C}} \mathrm{K_1} \xleftarrow[2.21\ \mathrm{kJ/mol}]{101\ ^\circ\mathrm{C}} \mathrm{K_2} \xleftrightarrow{40\ ^\circ\mathrm{C}} T_g$$

Table 1. Transition Enthalpy and Entropy Changes for Methylene Units and Mesogenic Groups for the Liquid Crystalline Transitions in TPP(n = odd)s and TPP(n = even)s

		ΔH, kJ/mol per repeating unit		ΔS, J/(K·mol) per repeating unit	
sample	transition	mesogen	methylene	mesogen	methylene
	I → N	1.64	9.45	2.80	23.1
	N → S_F	0.50	6.45	1.78	14.4
n = odd	I → S_F	2.14	15.9	4.58	37.5
	S_F → S_G	≈0.00	6.30	≈0.00	15.6
	S_G → S_H	≈0.00	13.8	≈0.00	35.3
	I → N	5.01	4.80	7.65	13.4
	N → S_F	7.15	1.92	11.43	8.76
n = even	I → S_F	12.2	6.72	19.14	21.7
	S_F → S_G	2.45	3.84	3.85	10.7
	S_G → S_H	≈0.00	11.4	≈0.00	27.0

for TPP($n = 12$). The transition temperatures (in °C) and their enthalpy changes (in kJ/mol) at each transition are also included. The entropy changes can be calculated using these two quantities ($\Delta h/T$) since these transitions are in thermodynamic equilibrium.[2,3]

Generally, the enthalpy and entropy changes of a liquid crystalline transition are critically dependent upon the structural rigidity, symmetry, planarity, and length of the mesogenic groups, all of which are essential to stabilize the liquid crystalline phase. Thus, it would be interesting to examine the individual contributions of the mesogenic groups and methylene units to the enthalpy and entropy changes at each phase transition temperature. These contributions may be obtained to a first approximation by a method recently employed for several main chain liquid crystalline polymers including a series of enantiotropic liquid crystalline (4,4′-dihydroxy-2,2′-dimethylazoxybenzene)-alkanedioic acids (ME9-Sn),[12] a series of monotropic liquid crystalline polyethers synthesized from 1-(4-hydroxyphenyl)-2-(2-methyl-4-hydroxyphenyl)ethane and odd-numbered α,ω-dibromoalkanes (MBPE-odd),[13] and a series of monotropic liquid crystalline poly(ester imide)s synthesized from *N*-[4-(chloroformyl) phenyl]-4-(chloroformyl)phthalimide and different diols (PEIM).[14] In this method, the relationships between the enthalpy and entropy changes are plotted with respect to the number of methylene units. Linear relationships can often be observed in a range of methylene units between $n = 4$ and 20.[2,3] The slopes of these linear relationships are thus representative of the contribution of each methylene unit to the enthalpy and entropy change, while the intercepts at $n = 0$ are representative of the contribution of the mesogenic groups to these two thermodynamic property changes at the transition temperatures. For the series of TPP(n = odd and even)s including TPP($n = 12$ and $n = 15$), the mesogenic group and methylene unit contributions to the enthalpy and entropy changes at each liquid crystalline phase transition temperature are listed in Table 1. The data will be used for comparison to the ^{13}C NMR results obtained from the methylene units in both polymers.

γ-Gauche Effect in ^{13}C NMR To Determine Methylene Conformations. Figure 1 shows the ^{13}C MAS spectra for TPP-12 measured at 190 °C (I), 180 °C (S_F), 150 °C (SC_G), 130 °C (SC_H), 110 °C (K_1), 90 °C (K_2), 70 °C (K_2), and 23 °C (glass) on cooling. Figure 2 shows the ^{13}C MAS NMR spectra on cooling for TPP-15 at 165 °C (I), 145 °C (S_F), 125 °C (SC_G), 90 °C (SC_H), 50 °C (SC_H), and 23 °C (glass). In the experiments, NMR data were collected at least twice, sometimes three times at

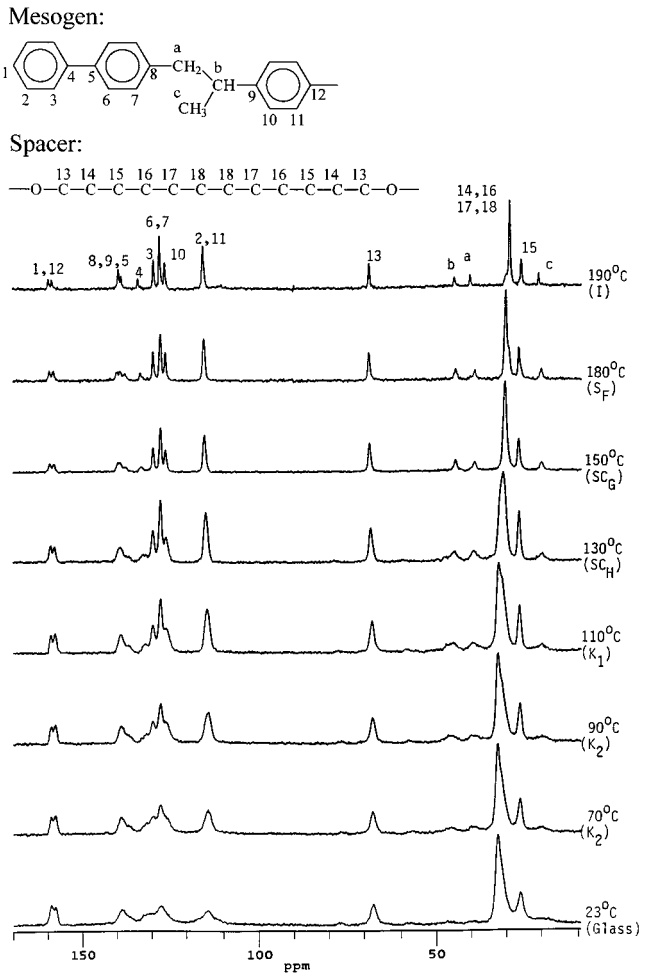

Figure 1. Variable-temperature solid-state ^{13}C MAS NMR spectra of TPP-12 and its molecular structure. The temperatures and phases are indicated on each plot. The numbers on the spectrum at 190 °C (melt) correspond to the numbers of the carbon atoms in the molecular structure.

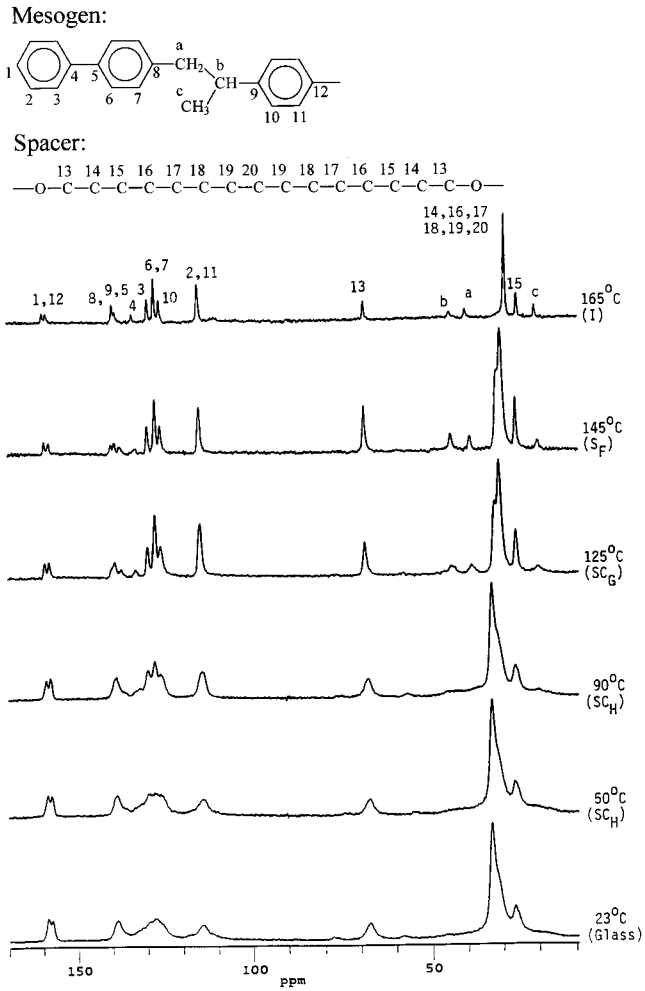

Figure 2. Variable-temperature solid-state ^{13}C MAS NMR spectra of TPP-15 and its molecular structure. The temperatures and phases are indicated on each plot. The numbers on the spectrum at 160 °C (melt) correspond to the numbers of the carbon atoms in the molecular structure.

each temperature in order to ensure reproducible results. Standard deviations from multiple data were found to be less than ±5%. The spectra of the isotropic melt, located at the top of Figures 1 and 2, show sufficient resolution for the ^{13}C NMR peak assignments. The peak assignments are made on the basis of model compounds and the additivity rules of substituent effects.[15,16] The numbers on the peaks in Figures 1 and 2 represent the carbon atoms as indicated in the molecular structures.

As shown in Figures 1 and 2, the resonances of the methylene carbon atoms are between 15 and 70 ppm. The most intense resonances between 23 and 37 ppm in these two figures are due to the central carbon atoms numbered 14 to 18 for TPP-12 (C14−C18) and 14 to 20 for TPP-15 (C14−C20). The carbon atoms numbered 13 and 15 (C13 and C15) show no change in their chemical shift as the temperature decreases from the isotropic melt to 23 °C. The remaining carbon atoms show a noticeable downfield shift with decreasing temperature (see expanded plots in Figures 3 and 4).

Under the conditions of magic-angle-spinning and dipolar decoupling of protons, the ^{13}C chemical shift possesses a conformational origin that has been described as the γ-gauche effect.[6−8] For a methylene segment of the alkyl chain in TPP, such as $-{}^{\gamma}CH_2CH_2-CH_2{}^{o}CH_2CH_2-CH_2{}^{\gamma}CH_2-$, the chemical shift of the carbon under observation, ^{o}C, is determined by the conformations of its two γ-substituents, $^{\gamma}C$ (rotational isomeric state). The *gauche* conformation causes more shielding on ^{o}C than the *trans*, and hence, an upfield shift in the ^{13}C NMR resonance is expected if the alkyl segment involves conformational disorder. However, the chemical shift changes can also be caused by the chain-packing effect, especially in molecules that have an *a priori* possibility of molecular motion as a whole or over a large portion of the molecule. Observations of such effects have also been made for solid polymers such as poly(3,3-diethyloxetane).[17] In the cases of TPP-12 and TPP-15, such interchain packing effects on the ^{13}C chemical shift of the spacer methylene carbons are probably not an important factor due to the fact that the mesogens are bulkier and, therefore, the methylene units sense less intermolecular interaction.

At temperatures above T_g, defined on the NMR time scale, it is more realistic that a mobile C−C bond assumes one of the two states dynamically. Namely, it is either in the *trans* conformation or undergoes an interconversion between the *trans* and the *gauche* conformations. While at temperatures below T_g, the conformations should be frozen into a distribution of conformations. For this reason, it is necessary to classify the carbon atoms in the methylene units into three categories. First, a carbon atom may have both γ-substituents in the *trans* conformation, which is designated as "*tt*". Second, a carbon atom may have one

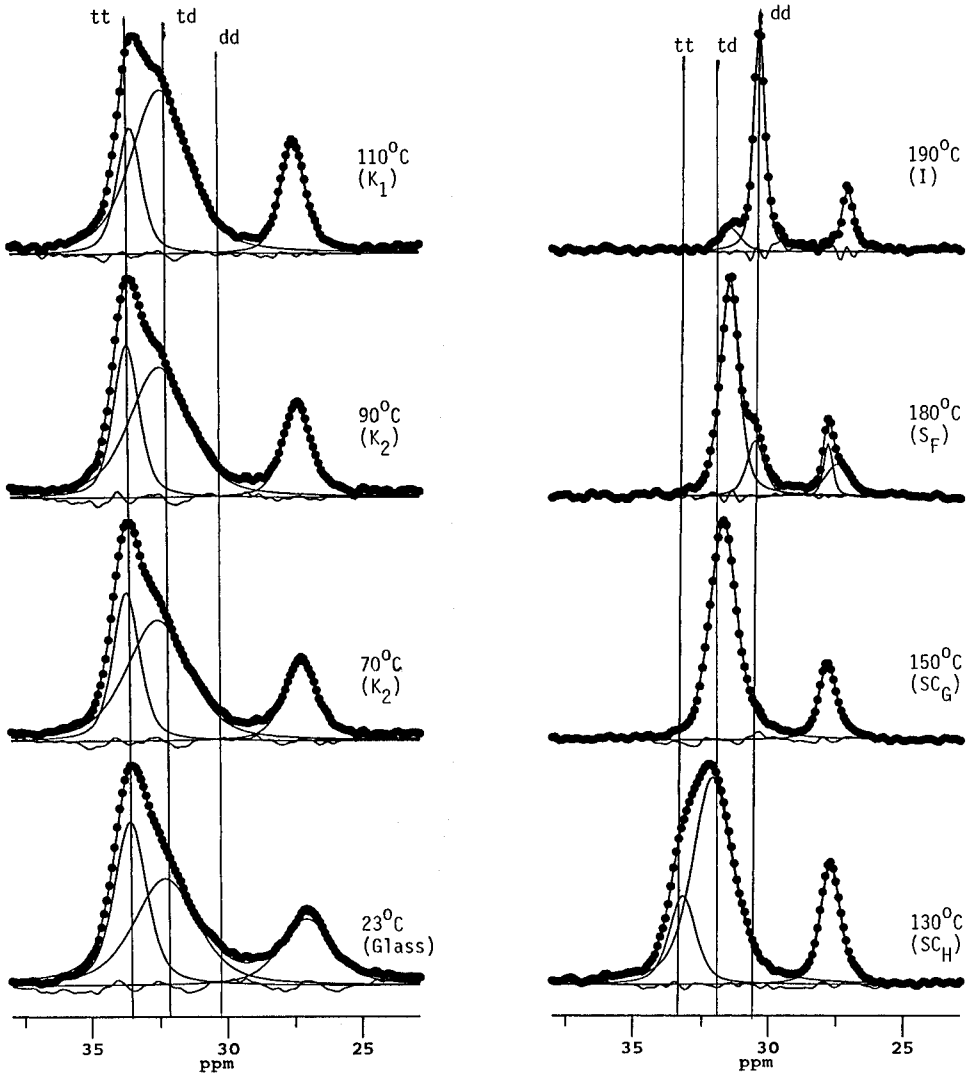

Figure 3. Expanded spectra for TPP-12 showing the resonances of all carbon atoms in the spacer, except C13. The dotted lines are the experimental data; the lines represent the line deconvolution results for the individual components, the sum, and the difference between the experimental and the sum. The three vertical lines indicate approximately the chemical shifts for carbon atoms in the "*tt*", "*td*", and "*dd*" arrangements.

γ-atom in the *trans* and the other in the dynamic interconversion process, which is designated as "*td*". Third, a carbon atom may have both γ-atoms dynamically disordered, which is designated as "*dd*". The following diagram illustrates the classification:

$$\overset{trans \quad * \quad trans}{CH_2CH_2-CH_2CH_2CH_2-CH_2CH_2} \qquad tt$$

$$\overset{trans \quad * \quad gauche}{CH_2CH_2-CH_2CH_2CH_2-CH_2CH_2} \qquad td$$

$$\overset{gauche \quad * \quad gauche}{CH_2CH_2-CH_2CH_2CH_2-CH_2CH_2} \qquad dd$$

Temperature Dependence of Methylene Conformations in TPPs. The chemical shift of C13 (*i.e.*, OCH_2), which is determined by the conformation of the bond between C14 and C15, has been found to remain constant (69 ppm) in the entire temperature region studied (from the isotropic melt temperature to room temperature), as shown in Figures 1 and 2. Since the conformation between C14 and C15 should be disordered in the isotropic melt and the chemical shift does not change in the temperature region studied, the C13 must thus be disordered over the entire temperature region. Thus, C13 should be identified as "*dd*". The same behavior is found for C15 for which the chemical shift (27 ppm) is independent of temperature (see Figures 3 and 4), indicating that the bonds of C13−C14 and C16−C17 are also disordered. Based on these arguments, a total of six bonds are disordered over the entire temperature region, as indicated in the following diagram

TPP-12 CH_2 units

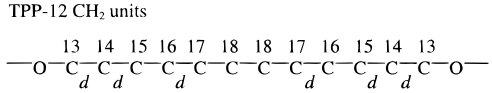

TPP-15 CH_2 units

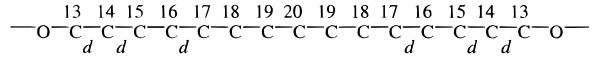

Analyses of the chemical shifts for the remaining carbon atoms, namely, C14, C16, C17, and C18 for TPP(n = 12) and C14, C16, and C17−C20 for TPP(n = 15), can be made on the basis of the results of line deconvolution and VCT experiments. Figures 3 and 4 show the expanded regions for the methylene carbons in TPP(n = 12 and 15) between 23 and 37 ppm. Since the resonances from the methylene carbons are partially overlapping, a deconvolution method based on confor-

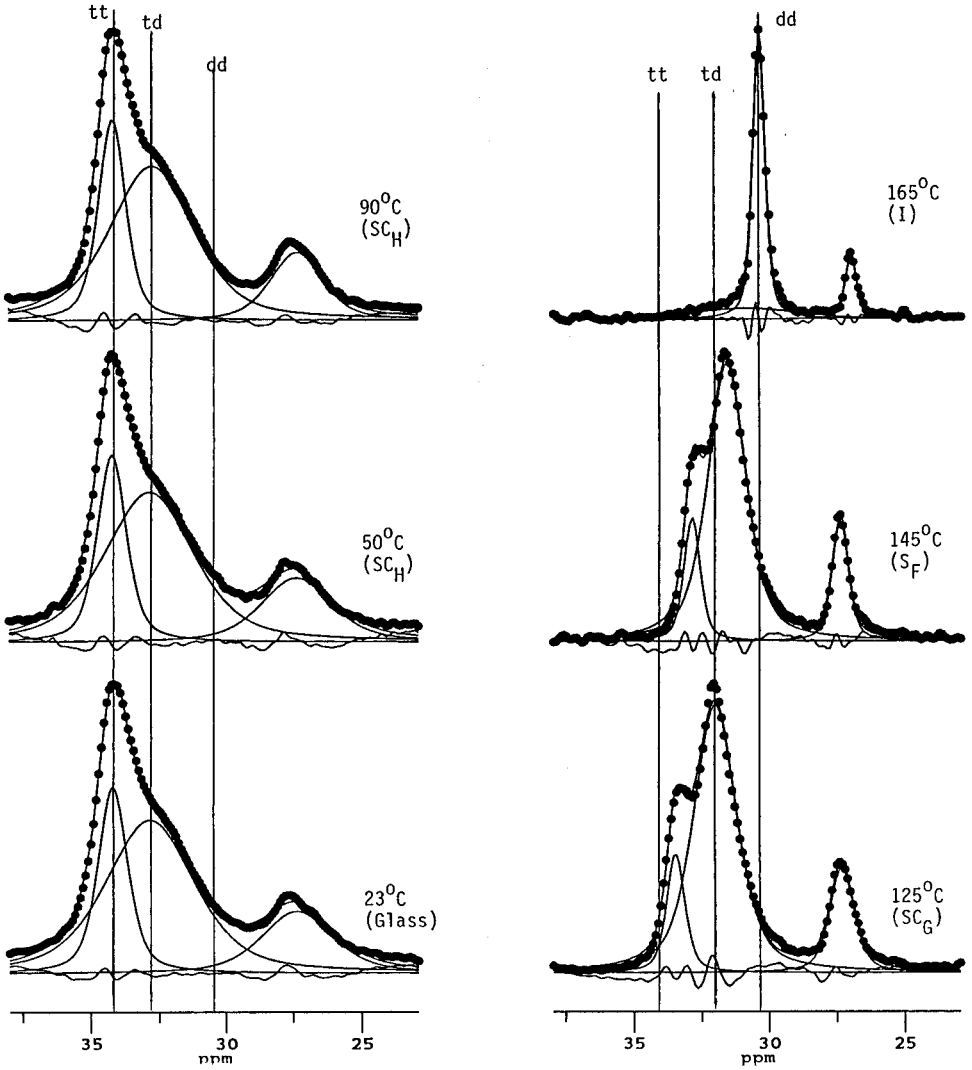

Figure 4. Expanded spectra of TPP-15 showing the resonances of all carbon atoms in the methylene units, except for C13. The dotted lines are the experimental data; the lines represent the line deconvolution results for the individual components, the sum, and the difference between the experimental and the sum. The three vertical lines indicate approximately the chemical shifts for carbon atoms in the "*tt*", "*td*", and "*dd*" arrangements.

mational arguments was performed. The dotted lines represent the experimental spectra, the solid lines represent individual components and the sum. The line shape used for each individual component is a combination of Gaussian and Lorentzian functions. The difference (residual) between the calculated sum of the deconvoluted individual components and the experimental spectra is also provided. A random variation of this difference close to a zero baseline indicates that the error follows a white noise (Gaussian) distribution with an expectation of zero. The peak positions of each component provide accurate values of the chemical shifts and are useful for the characterization of the chain conformation. The three vertical lines, labeled "*tt*", "*td*", and "*dd*", are provided in the figures to illustrate these three major conformational assignments found in the methylene units.

Based on the VCT experiments, the relationship between the signal intensity and contact time can be utilized to generate information on the maximum attainable signal intensity, which is related to the spin population:[18,19]

$$\mathbf{I} = I_0 \mathrm{e}^{-\tau/T_{1\rho H}} (1 - e^{-\tau/T_{CH}}) \qquad (1)$$

where τ is the contact time, I is the signal intensity at τ, I_o is the maximum static magnetization, which is proportional to the number of resonant ^{13}C spins, T_{CH} is the cross-polarization time constant, and $T_{1\rho H}$ is the ^1H spin−lattice relaxation time in the rotating frame. It should be noted that eq 1 is a simplified form of the rate equation for describing the signal intensity as a function of contact time. The justification of this simplification can be made if $T_{1\rho H} >> T_{CH}$. Table 2 lists typical values of $T_{1\rho H}$ and T_{CH} for TPP-12 and TPP-15 at different temperatures for the resonances of the "*tt*" and "*td*" arrangements, *i.e.*, about 34 and 32 ppm, respectively. As can be seen, the condition of $T_{1\rho H} >> T_{CH}$ is satisfied. The increase in T_{CH} as a function of temperature indicates the fact that the local molecular motion becomes faster and causes more effective averaging of the C−H heteronuclear dipolar interaction. The increase in $T_{1\rho H}$ with temperature is due to the increase of the rate of motion in the kilohertz range.

As we have discussed previously, the line deconvolution yields accurate chemical shift values while the VCT experiments provide a representation of the spin population (related to I_o in eq 1). Combining both observations permits a quantitative determination of the chain conformation of the methylene units. Table 3 lists the chemical shifts and associated signal intensities after the corrections were made on the basis of the VCT

Table 2. Values of $T_{1\rho H}$ and T_{CH} in TPP-12 and TPP-15 at Different Temperatures

temp, °C (phase)	peak "*tt*" (34 ppm)		peak "*td*" (32 ppm)	
	T_{CH} (ms)	$T_{1\rho H}$ (ms)	T_{CH} (ms)	$T_{1\rho H}$ (ms)
		TPP-12		
23 (glassy)	0.035	7.0	0.072	7.5
50 (K_2)	0.036	8.9	0.068	9.4
90 (K_2)	0.039	9.3	0.080	10.0
110 (K_1)	0.086	20.0	0.096	25.0
130 (SC_H)	0.68	37.3	0.75	40.0
150 (SC_G)	NA	NA	0.21	75.0
180 (S_F)	NA	NA	1.4	71.0
		TPP-15		
23 (glassy)	0.037	7.9	0.052	7.7
50 (SC_H)	0.042	8.6	0.055	9.1
90 (SC_H)	0.038	19.6	0.071	16.1
110 (SC_H)	0.045	18.6	0.093	26.0
125 (SC_G)	0.28	>100	0.38	>100
145 (S_F)	1.43	>100	1.53	>100

[a] The error bar of the reported values is equal to or less than 15%.

Table 3. ^{13}C NMR Results of the Methylene Units in TPP-12 and TPP-15 on Cooling

temp, °C (phase)	peak "*tt*"		peak "*td*"		peak "*dd*"		conf order
	δ_{tt} (ppm)	I_{tt}	δ_{td} (ppm)	$I_{td}I_{td}$	δ_{dd} (ppm)	I_{dd}	ρ
				TPP-12			
23 (glassy)	33.63	46.4	32.31	53.6	NA	0	0.76
70 (K_2)	33.76	35.1	32.62	64.9	NA	0	0.79
90 (K_2)	33.72	34.1	32.54	65.9	NA	0	0.77
110 (K_1)	33.60	25.3	32.50	74.7	NA	0	0.72
130 (SC_H)	33.21	22.1	32.10	77.9	NA	0	0.60
150 (SC_G)	NA	0	31.70	100	NA	0	0.41
180 (S_F)	NA	0	31.48	80.4	30.52	19.6	0.30
190 (Iso)	NA	0	31.38	15.3	30.33	84.7	0.071
				TPP-15			
23 (glassy)	34.19	30.0	32.85	77.0	NA	0	0.75
50 (SC_H)	34.19	30.5	32.86	69.5	NA	0	0.75
90 (SC_H)	34.19	30.9	32.76	69.1	NA	0	0.74
125 (SC_G)	33.48	16.3	32.03	83.7	NA	0	0.48
145 (S_F)	32.87	16.1	31.61	83.9	NA	0	0.36
165 (Iso)	NA	0	32.45	6.1	30.47	93.9	0.032

[a] See text and Figures 3 and 4 for the designations of "*tt*", "*td*", and "*dd*". [b] The *trans* content was calculated according to eqs 2 and 3, in which the chemical shifts and intensities are used as inputs.

experiments.

The carbon atoms can be characterized on the basis of the results of line deconvolution and VCT experiments shown in Table 3. The conformational order, ρ, for the methylene units can be empirically defined by the following expression:

$$\rho = I_{tt}F_{tt} + I_{td}F_{td} + I_{dd}F_{dd} \qquad (2)$$

where the I_{tt}, I_{td}, and I_{dd} are the corrected signal intensities (based on the cross-polarization time constant, T_{CH}, and proton spin−lattice relaxation time in the rotating frame, $T_{1\rho H}$) for the carbon atoms of "*tt*", "*td*", and "*dd*", respectively, and are given in Table 3. F_{tt}, F_{td}, and F_{dd} are weight factors based on the observed chemical shift values for the peaks "*tt*", "*td*", and "*dd*" and are defined as

$$F = \frac{\delta - \delta_{melt}}{\delta_{cryst} - \delta_{melt}} \qquad (3)$$

in which δ is the chemical shift value based on the line deconvolution results given in Table 3, δ_{melt} is the value measured from the isotropic melt (30.24 and 30.47 ppm for TPP-12 and TPP-15, respectively), which represents the result of rapid interconversion between *trans* and *gauche* conformations that occurs in the molten state, and δ_{cryst} is the chemical shift value for a perfect crystal of paraffin or polyethylene. The chemical shifts of the "*tt*" peak measured at 23 °C can be chosen for δ_{cryst} and are 33.77 and 34.19 ppm for TPP-12 and TPP-15, respectively. It should be pointed out that eq 2 is only a first-order approximation, *i.e.*, it links the conformational order (ρ) linearly with the chemical shift change. A better correlation could be developed on the basis of more rigorous calculations, for example, quantum-mechanical calculations, as suggested in the literature.[20] The conformational order, ρ, for the methylene units calculated according to eqs 2 and 3 are also listed in Table 3.

Figures 3 and 4 show the resonances of remaining methylene carbon atoms between 35 and 29 ppm, *i.e.*, C14, C16, C17, and C18 for TPP-12 and C14 and C16−C20 for TPP-15. Below the isotropization temperature, there are only two components that can be identified as "*tt*" and "*td*", having typical chemical shifts of 34 and 32 ppm, respectively. At the isotropization temperature, two components exist that can be identified as "*td*" and "*dd*" with typical chemical shifts of 32 ppm and 30.5 ppm, respectively. It is clear that the chemical shifts decrease in going from "*tt*" to "*td*" and to "*dd*", because the disordering causes an upfield shift (smaller chemical shift values) due to the γ-gauche effect.

It is interesting that in all highly ordered smectic and smectic crystal phases (S_F, SC_G, and SC_H), the methylene carbon atoms are mainly in the "*td*" arrangement, with a minor fraction of "*tt*". The "*dd*" arrangement (20%) can only be found in the S_F phase of TPP($n = 12$). In this sample the content of "*tt*" arrangements is virtually zero. In the case of the SC_G phase of this polymer, the "*td*" arrangement is the only conformational feature aside from C13 and C15 that remain as "*dd*" at all temperatures. With increasing order, the concentration of "*tt*" arrangement increases at the expense of the "*td*" arrangement. For TPP($n = 15$) the content of "*dd*" conformation is practically zero below the isotropization temperature. This is in contrast to the amorphous phase of polyethylene in which the ^{13}C chemical shift is found to be between 31.0 and 30.1 ppm depending on the temperature and should be more appropriately assigned to the "*dd*" arrangement. On the other hand, a weak "*td*" component is evident even in the isotropic state of TPP($n = 15$), suggesting that the methylene units retain some conformational order even in the melt.

It should also be pointed out that we assume single-phase behavior in all of these highly ordered smectic phases. This is a reasonable assumption based on the results of thermodynamic properties and phase morphological observations reported in these polyethers.[1−3] Other reports have shown that in some polymer systems different phases may coexist.[21,22]

Correlation with the Entropy Change Data. The total entropy change for the methylene units in TPP($n = 12$) between the isotropic melt and SC_H phases is 59.4 J/(K mol), while that in TPP($n = 15$) is 88.4 J/(K mol). From the isotropic melt to the SC_H phase, the overall entropy change for each methylene unit in TPP($n = 15$) is higher than that in TPP($n = 12$). This indicates that the role of the methylene units in TPP(n = even)s and TPP(n = odd)s differs with respect to stabilization of

Table 4. Comparison of Methylene Unit Contributions to the Entropy Changes and Conformational Order at Liquid Crystalline Transitions

transitions	$\Delta S/\Delta S(I \leftrightarrow SC_H)$	$\Delta\rho/\Delta\rho(I \leftrightarrow SC_H)$
	TPP-12	
$I \leftrightarrow S_F$	37%	43%
$S_F \leftrightarrow SC_G$	18%	21%
$SC_G \leftrightarrow SC_H$	45%	36%
	TPP-15	
$I \leftrightarrow S_F$	42%	46%
$S_F \leftrightarrow SC_G$	17%	17%
$SC_G \leftrightarrow SC_H$	42%	38%

the liquid crystalline phase. It is possible to correlate the number of bonds that change their conformation from the *trans* to the disordered state with the transition entropy changes. From the NMR results, the changes in the conformational order, ρ (in Table 3), between the SC_H and the isotropic melt are 60.0% − 7.1% = 52.9% for TPP-12; and 75.0% − 3.2% = 71.8% for TPP-15. It is thus possible to calculate the percentage of the entropy change and the percentage of the conformational order change at each transition. They are listed in Table 4. From Table 4, it is clear that the percentages based on both the entropy change from DSC and the conformational order change from NMR show rough correspondence. A tendency is found in both polymers for overestimation of the $I \leftrightarrow S_F$ transition and underestimation of the $SC_G \leftrightarrow SC_H$ transitions by NMR. This is particularly true in the case of TPP(n = 12). Deviation may arise due to the approximation used in eqs 2 and 3, which may insufficiently describe these changes using an additive scheme. In addition, although the conformational contribution is the major part of the entropy change during the transition, other minor contributions such as volume changes at the transition may also be attributed to the overall entropy change. The deviations observed for the transitions, however, do not invalidate the qualitative agreement between DSC and the method based on the evaluation of conformational order.

Conformation of Mesogenic Groups. The liquid crystalline behavior of TPP-n is partially due to the rodlike geometry and inflexibility of the mesogenic group 1-(4-hydroxy-4′-biphenylyl)-2-(4-hydroxyphenyl)-propane. The geometry and rigidity requirements are satisfied only if the rotation about the single bond C_a-C_b is restricted. The rigidity of the mesogenic unit is facilitated by the side group $-CH_3$ (C_c) due to the steric effect. In the aromatic part of MBPE[9] and HPX-C11,[10] such a side group is absent and conformational disordering in the mesogenic unit is possible below the isotropization temperature. The ^{13}C NMR spectra shown for TPP-12 and TPP-15 in Figures 1 and 2 indicate that the signals from C_a, C_b, and C_c are much broader than all others in the entire temperature region. The plausible explanation for this line-broadening is due possibly to a hindrance that prohibits the conformational isomerism about C_a-C_b below isotropization and slows down the small degree of rotational freedom around the C_a-C_b band to a rate comparable to the frequencies of coherent averaging, i.e., proton dipolar decoupling (50 kHz) or magic angle spinning (4 kHz). Thus, the entropy contribution from the mesogenic units contains not only the orientational disordering but also a conformational disordering of C_a-C_b in TPP-12 and TPP-15.

Conclusion

The motion and conformation of TPP-12 and TPP-15 polyethers have been characterized by solid state ^{13}C NMR under the conditions of magic angle spinning and dipolar decoupling of protons. The γ-gauche effect was employed to probe the conformational change associated with the flexible spacer as a function of temperature. It could be demonstrated that the methylene units in the polyethers assume partial conformational order in all of the liquid crystalline states. The "*td*" arrangement in the methylene units is the major conformation in the mesophase, and the minor arrangement of "*tt*" segments is less than 30%. The completely disordered state, characterized by the "*dd*" arrangement, can only be observed in the isotropic state.

Acknowledgment. This work was partially supported by Division of Materials Research, the National Science Foundation (DMR-9617030) and NSF Science and Technology Center for Advanced Liquid Crystalline Optical Materials (DMR-8920147).

References and Notes

(1) Cheng, S. Z. D.; Yoon, Y.; Zhang, A.; Savitski, E. P.; Park, J.-Y.; Percec, V.; Chu, P. *Macromol. Rapid Commun.* **1995**, *16*, 533.
(2) Yoon, Y.; Zhang, A.; Ho, R.-M.; Moon; B.; Cheng, S. Z. D.; Percec, V.; Chu, P. *Macromolecules* **1996**, *29*, 294.
(3) Yoon, Y.; Ho, R.-M.; Moon, B.; Kim, D.; McCreight, K. W.; Li, F.; Harris, F. W.; Cheng, S. Z. D.; Percec, V.; Chu, P. *Macromolecules* **1996**, *29*, 3421.
(4) Ho, R.-M.; Yoon, Y.; Leland, M.; Cheng, S. Z. D.; Yang, D.; Percec, V.; Chu, P. *Macromolecules* **1996**, *29*, 4528.
(5) Ho, R.-M.; Yoon, Y.; Leland, M.; Cheng, S. Z. D.; Percec, V.; Chu, P. *Macromolecules* **1997**, *30*, 3349.
(6) Grant, M.; Cheney, B. V. *J. Am. Chem. Soc.* **1967**, *89*, 5315.
(7) Tonelli, A. E.; Schilling, F. C.; Bovey, F. A. *J. Am. Chem. Soc.* **1984**, *106*, 1157.
(8) Tonelli, A. E. *NMR Spectroscopy and Polymer Microstructure, The Conformational Connection*; VCH Publishers: New York, 1989.
(9) Cheng, J.; Jin, Y.; Wunderlich, B.; Cheng, S. Z. D.; Yandrasits, M. A.; Percec, V. *Macromolecules* **1992,** *25*, 5991.
(10) Cheng, J.; Jin, Y.; Chen, W.; Wunderlich, B.; Gedde, Ulf W. *J. Polym. Sci., Part B: Polym. Phys.* **1994**, ***32***, 721.
(11) Percec, V.; Chu, P.; Ungar, G.; Cheng, S. Z. D.; Yoon, Y. *J. Mater. Chem.* **1994**, *4*, 719.
(12) Blumstein, A.; Thomas, O. *Macromolecules* **1982**, *15*, 1264. See also: Blumstein, B.; Stickles, E. M.; Blumstein, A. *Mol. Cryst. Liq. Cryst.* **1982**, *82*, 205. Blumstein, B.; Blumstein A. *Mol. Cryst. Liq. Cryst.* **1988**, *165*, 361.
(13) Yandrasits, A.; Cheng, S. Z. D.; Zhang, A.; Cheng, J.; Wunderlich, B.; Percec, V. *Macromolecules* **1992**, *25*, 2112.
(14) Pardey, R.; Shen, D.; Gabori, P. A.; Harris, F. W.; Cheng, S. Z. D.; Adduci, J.; Facinelli, J. V.; Lenz, R. W. *Macromolecules* **1993**, *26*, 3687.
(15) Silverstein, M.; Bassler,G. C.; Morrill, T. C. *Spectrometric Identification of Organic Compounds*; John Wiley & Sons: New York, 1981.
(16) Stothers, B. *Carbon-13 NMR Spectroscopy*; Academic Press: New York, 1972.
(17) Gomez, M. A.; Cozine, M. H.; Schilling, F. C.; Tonelli, A. E.; Bello, A.; Fatou, J. G. *Macromolecules* **1987**, *20*, 1761.
(18) Jelinski, L. W.; Melchior, M. T. In *NMR Spectroscopy Techniques*; Dybowski, C., Lichter, R. L., Eds.; Marcel Dekker: New York, 1987.
(19) Mehring, M. *High Resolution NMR in Solids*, 2nd ed.; Springer-Verlag: Berlin, 1983.
(20) Seidman; Macial, G. E. *J. Am. Chem. Soc.* **1977**, *99*, 659.
(21) Schmidt-Rohr, K.; Clauss, J.; Spiess, H. W. *Macromolecules* **1992**, *25*, 3273.
(22) Kricheidorf, H. R.; Probst, N.; Schwarz, G.; Wutz, C. *Macromolecules* **1996**, *29*, 4234.

MA970177M